Journal Pre-proof

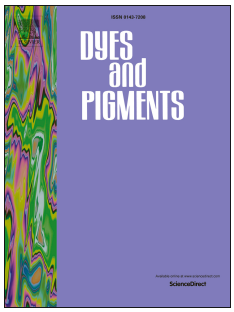

A styrylpyridinium dye as chromogenic and fluorogenic dual mode chemosensor for selective detection of mercuric ion: Application in bacterial cell imaging and molecular logic gate

Madhusmita Tripathy, Usharani Subuddhi, Sabita Patel

PII: S0143-7208(19)32377-0

DOI: https://doi.org/10.1016/j.dyepig.2019.108054

Reference: DYPI 108054

To appear in: *Dyes and Pigments*

Received Date: 10 October 2019

Revised Date: 12 November 2019

Accepted Date: 16 November 2019

Please cite this article as: Tripathy M, Subuddhi U, Patel S, A styrylpyridinium dye as chromogenic and fluorogenic dual mode chemosensor for selective detection of mercuric ion: Application in bacterial cell imaging and molecular logic gate, *Dyes and Pigments* (2019), doi: https://doi.org/10.1016/j.dyepig.2019.108054.

Table of contents entry

The styrylpyridinium D-π-A chromophore L1 exhibits selective and reversible binding to Hg^{2+} with visual and turn-on fluorescence response along with possibilities of intracellular imaging applications.

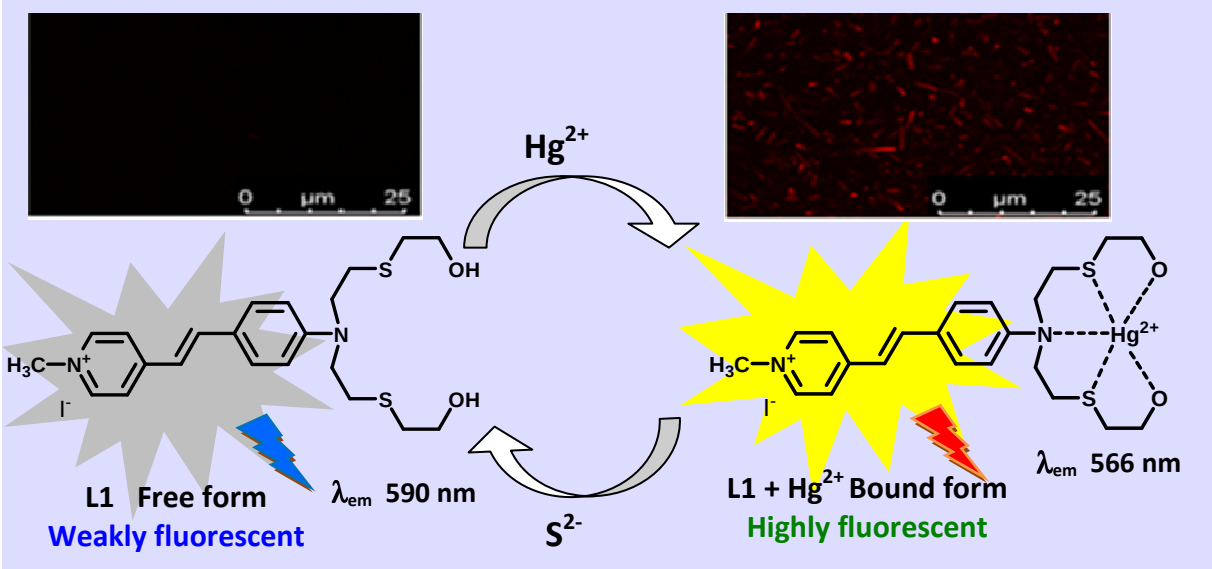

A styrylpyridinium dye as chromogenic and fluorogenic dual mode chemosensor for selective detection of mercuric ion: Application in bacterial cell imaging and molecular logic gate

Madhusmita Tripathy, Usharani Subuddhi and Sabita Patel*

Department of Chemistry

National Institute of Technology Rourkela, Odisha, India-769008

Email: sabitap@nitrkl.ac.in; Ph: +91-6612462660

Abstract

The present work demonstrates design, synthesis and chemosensing application of a styrylpyridinium based donor-π-acceptor (D-π-A) chromophore (L1) containing NS_2O_2 binding site. The chemosensor L1 selectively and successfully detects Hg^{2+} ions both visually and spectro-photometrically in perfect aqueous medium as well as in an aqueous-alcoholic mixture. Contrary to the reported literature on mercury sensing by cyanine dye which were reported to be "turn-off" Hg^{2+} sensor, probe L1 shows fluorescence "turn-on" response. D-π-A chromophore L1 exhibits orange colour in aqueous and aqueous-alcoholic solution due to intramolecular charge transfer (ICT) from the N, N-disubstitutedaminostyryl donor to pyridinium acceptor moiety. It shows Hg^{2+}-specific colour change with concomitant generation of a new absorption band and large emission enhancement (~ 10 fold) along with a blue shift of emission peak, owing to the formation of a selective 1: 1 L1-Hg^{2+} complex. ^{1}H-NMR analysis reveals the binding mode of L1 with Hg^{2+}. Hg^{2+} probing process was found to be reversible in presence of sulphide anion. The reversible off-on-off fluorescence response of the sensor with Hg^{2+} and S^{2-} has been used to generate an INHIBIT molecular logic gate. The probe not only provides a highly efficient, low cost, portable sensor for recognition and naked-eye detection of Hg^{2+} with a low detection limit in aqueous solution but its turn-on fluorescence response and cell permeability offer the possibility of using it for fluorescence imaging in living cells.

Keywords: Styrylpyridinium dye, Chemosensor, Mercuric ion, ICT, Fluorescence, D-π-A chromophore

1. Introduction

The recognition and sensing of metal ions has become increasingly important and emerged as a significant goal in the field of chemical sensors due to their biological, medicinal, and environmental hazardous impact.[1-4] Traditional analytical techniques such as high-performance liquid chromatography, mass spectrometry, atomic absorption spectroscopy, inductively coupled plasma atomic emission spectrometry, electrochemical sensing, *etc.* used to analyze the target provide accurate result, however associated with multiple shortcomings including extensive and time-consuming procedures, involve the use of sophisticated instrumentation and requirement of large size sample. In this regard, chromogenic and fluorogenic techniques by the use of chromoionophoric sensors have emerged as promising alternatives in recent years for the sensing of ions and small molecules of biological and environmental relevance.[1-4] Owing to a range of advantages *e.g.* high sensitivity, selectivity, operational simplicity, economical perspective, minimal and cheaper instrumental assistance, naked-eye detection, quantitative estimation of analytes, variety of chromoionophoric chemosensors are being designed and developed.[5-8] Chromoionophoric sensors comprise of two essential features (i) an ionophore with a specific binding pocket for selective recognition and binding of ions and (ii) at least one chromophoric or fluorophoric moiety capable of transducing the chemical information produced by the ionophore-ion interaction into an resolvable distinct optical signal either through change in colour or through change in fluorescence response.[5-10]

Mercury is found to be one of the most common pollutants and highly toxic heavy metal ion. Both elemental and ionic mercury present in soil and water are methylated by microorganisms and the resultant methylmercury is subsequently bio-accumulated through food chain.[11]Organomercury compounds, easily permeated through the cell membrane and able to reach high levels in the central nervous system (CNS), leading to nephrological and neurological dysfunctions. The direct chemical interaction between methylmercury and thiol groups from proteins and non-protein molecules, such as glutathione (GSH), is one of the major pathways in mercury induced neurotoxicity.[12] Hence, the sensitive and selective detection of mercury in biological and environmental samples is very important and highly desirable. Numerous reports on design and development of chromogenic and fluorogenic chemosensors for selective binding and detection of Hg^{2+} ion are found in literature. However, presence of Hg^{2+} ion significantly quenches the fluorescence signal through spin-

orbit coupling making them less useful for practical purpose.[13] Therefore, sensors which display "turn-on" response upon binding with metal ions are mostly preferred. In the designing of turn-on sensors for Hg^{2+}, an important strategy is to incorporate covalently binding donor atoms (particularly S-Donor atoms) in the binding site of potential sensor. These covalently bound donor atoms strongly interact with Hg^{2+}, weaken the interaction of the heavy metal with the fluorophore and thus facilitate to resume fluorescence.[13]

With a view to get selective "turn-on" chemosensor for mercury atom, the greater binding affinity of mercury towards sulphur atom is considered. In this regard a thioether based metal binding unit containing NS_2O_2 donor atoms is appended with a styrylpyridinium chromophore. Styrylpyridinium dyes are a class of polymethine hemicyanine dyes, well known for their applications in diverse and broad area of science, technology, engineering, pharmacology and medicine.[14-19] These dyes possess excellent electronic properties due to easy electronic delocalization, and found to exhibit electronic transition in the visible and NIR region of the electromagnetic spectrum.[20-22] Labelling of proteins, DNA, and other biopolymers with polymethine dye molecules, has become a very powerful research tool in molecular biology to unveil various biological and biochemical processes.[23] Notable use of these dyes in biology, medicine and drug development are as fluorescent probes and labels for cells, micelles and organelles, flow cytometry, fluorescence microscopy, DNA sequencing, detection on microarrays, quantification of nucleic acids in capillary and gel electrophoresis and single molecule detection of DNA. Considering numerous advantages of polymethine styrylpyridinium framework such as aqueous solubility, stability, long absorption and emission wavelength, high extinction coefficient and fluorescence quantum yield, uses in two-photon absorption, low detection limit and most importantly their cell permeability, non toxicity at low micro-molar level and cell imaging, herein we have reported the chromoionophoric application of a styrylpyridinium dye (L1) **(Scheme 1)** in aqueous and aqueous-alcoholic mixture. Probe L1 is designed to have a Donor-π-Acceptor framework and characterized with intramolecular charge transfer (ICT) from the N,N-disubstitutedaminostyryl donor to N-alkylpyridinium acceptor. Presence of pyridinium unit made it highly soluble in aqueous medium. The chemosensor was found to display high selectivity and sensitivity for Hg^{2+} in both water and water-ethanol mixture irrespective of other interfering ions. This is attributed to the strong binding interaction of Hg^{2+} with NS_2O_2 donor ligand as compared to other metal ions. The selective binding of the metal ion could be easily detected by "naked-eye" colour change, UV-Vis spectral change and through

fluorescence "turn-on" response. The significant fluorescence enhancement (~10-fold) was attributed to chelation enhanced fluorescence (CHEF) due to the arrest of excited state photo electron transfer (PET), decreased nonradiative relaxation and increased conformational rigidity as a result of the binding of metal ion with the donor atoms. Contrary to the reported literature on mercury sensing of styryl based dye chromophore which were reported to be "turn-off" Hg^{2+} sensor, probe L1 showed fluorescence "turn-on" response.[24-26] Exploiting this advantage of turn-on response for Hg^{2+} along with the water solubility, low toxicity and cell permeability of styrylpyridinium dyes, probe L1 was used for fluorescence imaging of Hg^{2+} in bacterial cell. Further, reversible fluorescence response in presence of sulphide anion was applied to construct an INHIBIT molecular logic gate.

2. Experimental Section

General materials and methods

All the solvents and reagents (analytical grade and spectroscopic grade) were obtained commercially and used after purification. Reactions were monitored by TLC, and the residue was chromatographed on a silica gel (100–200 mesh), using ethyl acetate-petroleum ether mixture as eluent. Melting point of solid samples was monitored on Yanaco Melting Point Apparatus SP-500. All NMR spectra were recorded on a Bruker Spectrometer 400 MHz (for ^{1}H NMR) and 100 MHz (for ^{13}C NMR) NMR spectrometer, and chemical shifts were expressed in δ ppm units relative to the TMS signal (as an internal reference), to $CDCl_3$ taken as 7.28 ppm for ^{1}H and 77.00 ppm for ^{13}C or to DMSO-d_6 taken as 2.5 ppm for ^{1}H NMR. UV-vis absorption spectra were recorded on a double beam Shimadzu (UV-1800) spectrophotometer using a quartz cuvette (path length = 1 cm). IR spectra were recorded using a Shimadzu IR Affinity-1 SWL using thin film deposit on KBr plates. High resolution mass spectra (HRMS) were acquired on a Bruker ESI-MS micro TOF-QII mass spectrometer. Fluorescence measurements were performed using FluoroMax-4P fluorescence spectrometer (HORIBA Scientific, USA) and a quartz cell (1 cm x 1 cm). Fluorescence lifetime measurements were carried out using IBH 5000F Nano LED equipment (Horiba Jobin Yvon, Edison, NJ) with Data Station software in the time-correlated single photon counting (TCSPC) mode. The method for determination of fluorescence quantum yield and lifetime is presented in electronic supporting information (ESI).

*Synthesis of 4-[N,N-Bis(2-chloroethyl)amino]benzaldehyde (**2**)*

Compound 2 was synthesized using a method reported in literature.[27] 20 ml of dimethylformamide was placed in a 100 ml flask equipped with a mechanical stirrer and cooled to 0-5° as 10 ml of phosphorus oxychloride was added slowly over approximately 0.5 hr. A solution containing 3.62 g (20 mmol) of N, N-bis(2-hydroxyethyl) aniline was then added with stirring and cooling. After stirring at 90° C for 2.5 hr, the mixture was cooled and poured into 200 m1 of ice cold water. Concentrated ammonium hydroxide was then added with vigorous stirring until the solution was strongly basic as checked by pH paper. The solid yellow product precipitated was then collected and recrystallized from methanol-water to give 1.73 g (59% yield) of the cream colored needles (M.Pt. 85-88° C). ^{1}H NMR (400 MHz, $CDCl_3$) δ (ppm): 9.80 (s, 1H), 7.81 (d, J = 9.2 Hz, 2H), 6.77 (d, J = 8.8 Hz, 2H), 3.88 (t, J = 13.6 Hz, 4H), 3.72 (t, J = 13.6 Hz, 4H) (Figure S1: Electronic supporting Information (ESI)) ^{13}C NMR (100 MHz, $CDCl_3$) δ (ppm): 190.2, 150.9, 132.3, 126.7, 111.2, 77.0, 53.3, 40.0 (Figure S2: ESI).

*Synthesis of 4-(N,N-bis-(2-hydroxyethylthioethyl))benzaldehyde (**3**)*

Compound **3** was prepared as per the following procedure.[27] Na metal (0.2 g, 10 mmol) was added into ethanol (5.6 ml) along with stirring. After Na reacted completely, 2-mercaptoethanol (0.7 ml, 10 mmol) was added into the solution with stirring for 1 hr at room temperature. Solution of **2** (1.23 g, 5 mmol) in 2.5 ml DMF was then added in portions. After stirring for 1 hr, the mixture was then stirred at 60 ^{0}C for another 1hr. The reaction mixture was then diluted with water and was extracted with DCM (6 x 10 ml) and dried over Na_2SO_4. DCM was then removed from the mixture in a rotary evaporator and residue was vacuum dried. The desired product was found as brown colored viscous oil 1.32 g (78% yield). ^{1}H NMR (400 MHz, $CDCl_3$), δ : 9.74 (s, 1H), 7.76 (d, J = 8.8 Hz, 2H), 6.72 (d, J = 9.2 Hz, 2H), 5.31(s, 2H), 3.82 (t, J = 12 Hz, 4H), 3.69 (t, J = 15.2 Hz, 4H), 2.83 (m, J = 12 Hz, 8H) (Figure S3: ESI).; ^{13}C NMR (100 MHz, $CDCl_3$) δ: 190.2, 151.4, 132.4, 125.9, 111.4, 77.0, 61.2, 51.4, 35.4, 29.1 (Figure S4: ESI).; HRMS: m/z $[M+Na]^+$ 352.1034 (Calcd); Found: 352.1012 (Figure S5: ESI).; IR(KBr): 3373, 2920, 1654, 1595, 1523, 1402, 1288, 1168, 1045, 945, 817cm^{-1} (Figure S6: ESI).

*Synthesis of (E)-4-(4-N,N-bis-(2-hydroxyethylthioethylamino)styryl)-1-methylpyridinium iodide (**L1**)*

The Compound **3** (0.658 g, 2 mmol) and 1,4-dimethylpyridinium iodide (0.220 g, 2mmol) were mixed in 6 ml of absolute ethanol in presence of 1 drop of piperidine as base catalyst. The resulting mixture was heated to reflux overnight. After cooling, the mixture was filtered to collect the solid followed by washing with ethanol. The crude product was recrystallized twice from ethanol and then dried in vacuum to obtain red colored chemosensor 0.27 g (56% yield) m.pt. 139-141^{0}C. ^{1}H NMR (400 MHz, DMSO-d_6) δ (ppm) : 6.76-8.68 (m, 8H), 7.18 (d, J = 16 Hz, 1H), 7.91 (d, J = 16 Hz, 1H), 4.87 (s, 1H), 4.17 (s, 3H), 3.60 (m, J = 13.2 Hz, 8H), 2.76 (t, J = 14 Hz, 4H), 2.68 (t, J = 13.2 Hz, 4H) (Figure S7: ESI).; ^{13}C NMR (100 MHz, DMSO-d_6), δ (ppm): 153.7, 149.4, 144.8, 130.9, 123.1, 117.7, 112.1, 61.6, 51.0, 46.8, 40.1, 39.2, 34.5, 29.1 (Figure S8: ESI).; HRMS: m/z $[M]^+$ 419.1841(Calcd); Found: 419.1821 (Figure S9: ESI). ; IR (KBr): 3296, 2918, 1645, 1585, 1523, 1404, 1340, 1172, 1045, 972, 945, 827cm^{-1} (Figure S10: ESI).

3. Results and Discussion

*Synthesis of chemosensor 4-(4-N,N-bis-(2-hydroxyethylthioethylamino)styryl)-1-methylpyridinium iodide (**L1**)*

The chemosensor **L1** was synthesized by a simple condensation reaction of 1,4-dimethylpyridinium iodide (**4**) and 4-(N,N-bis-(2-hydroxyethylthioethyl))aminobenzaldehyde (**3**) in presence of piperidine in ethanolic medium to form the styrylpyridium dye **L1 (Scheme 1)**. Formation of the product was characterized from IR, NMR (^{1}H and ^{13}C) and mass spectral analysis (Figure S7 –S10; ESI).

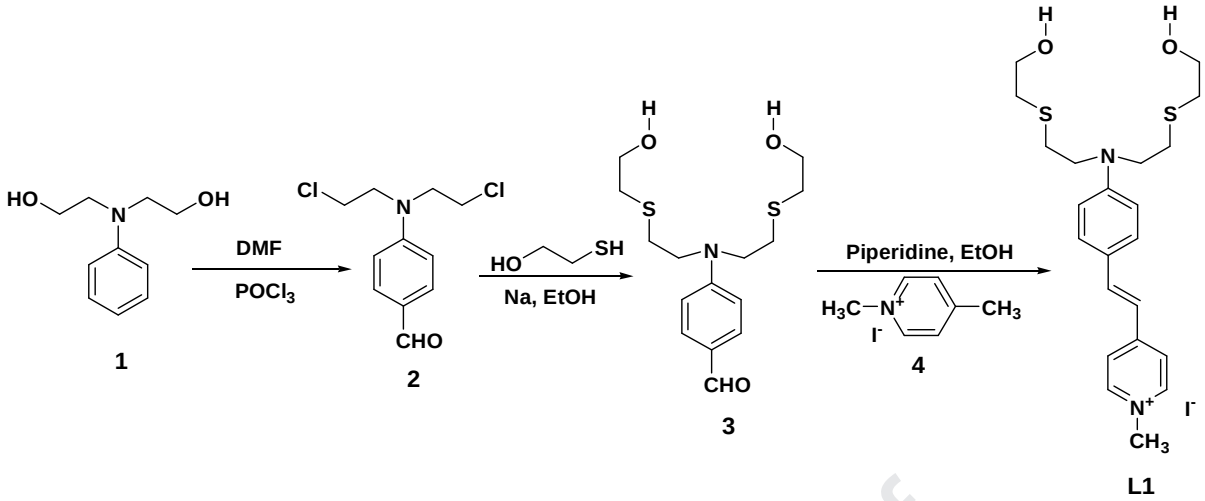

Scheme 1 The stepwise synthetic route to chemosensor **L1**.

*Solvatochromism of the probe **L1***

Styrylpyridinium dyes, a class of polymethine hemicyanine dyes are very well known for their solvent-induced reversible colour change termed as solvatochromism.[20, 28-30] Due to the presence of Donor-π-Accepter (D-π-A) moiety, upon excitation these molecules exhibit a large change in dipole moment attributed to the relative contributions of both benzenoid and quinonoid forms. Extensive study on the solvatochromism/fluorosolvatochromism of different classes of polymethine dyes proved their sensitivity to environmental changes and thus used as good probes for monitoring micropolarity, hydrogen bonding interactions, and for the investigation of micro-environmental characteristics of biochemical and biological systems.

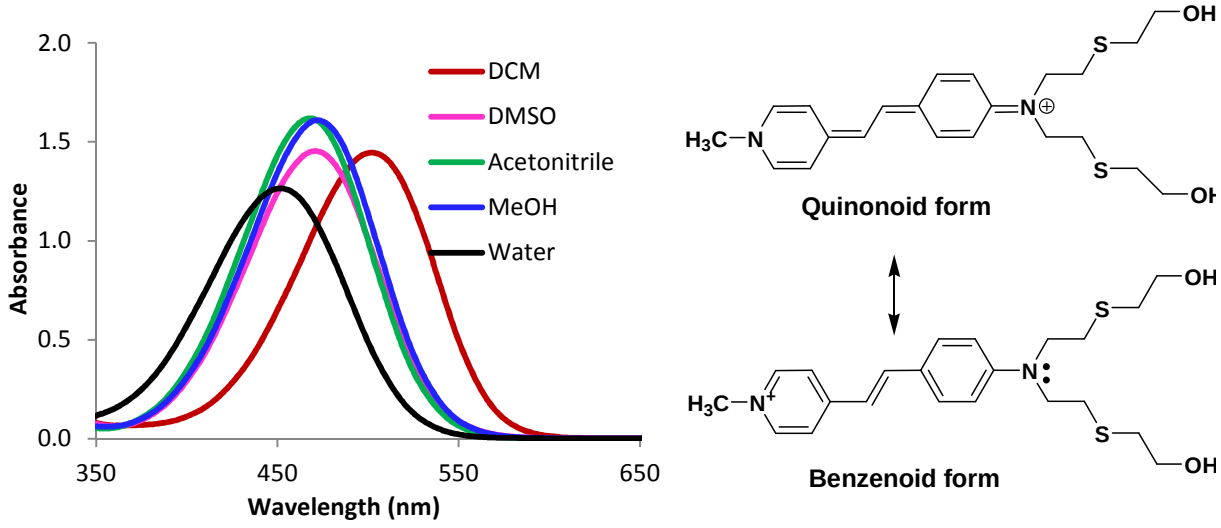

Figure 1 ICT absorption band of styrylpyridinium dye **L1** in different solvents

The styrylpyridinium chemosensor **L1**, contains a D-π-A chromophore with conjugated tertiary nitrogen groups as the donor and quaternary pyridinium nitrogen centre as the acceptor, flanked with styryl π-spacer. The large solvatochromic shift (i.e 450 nm in water to 503 nm in dichloromethane (DCM)) clearly demonstrates intra molecular charge transfer (ICT) characteristic of the chromophore (Figure 1).

Chromoionophoric evaluation

The aqueous solubility of the chemosensor **L1** made it possible to study its metal ion binding efficacy in aqueous as well as in aqueous-alcoholic medium. The binding properties of the probe **L1** with Hg^{2+} and with other metal ions were studied by naked eye visualisation test as well as UV-Vis and fluorescence emission experiments in water and in MeOH-H_2O (4:1 v/v) mixture. Figure 2 depicted the visual change on adding 4 equivalents of different metal ions (4.8×10^{-5} M) to the solution of **L1 (**1.2×10^{-5} M) in water medium. Orange solution of probe **L1** became colourless with mercury ion, however in presence of other tested metal ions it remained unaffected when observed in daylight. Similarly, under the influence of UV light strong yellow fluorescence was observed only with Hg^{2+} ion. This clearly demonstrated the chromoionophoric chemosensor nature of the compound **L1** for selective detection of Mercury.

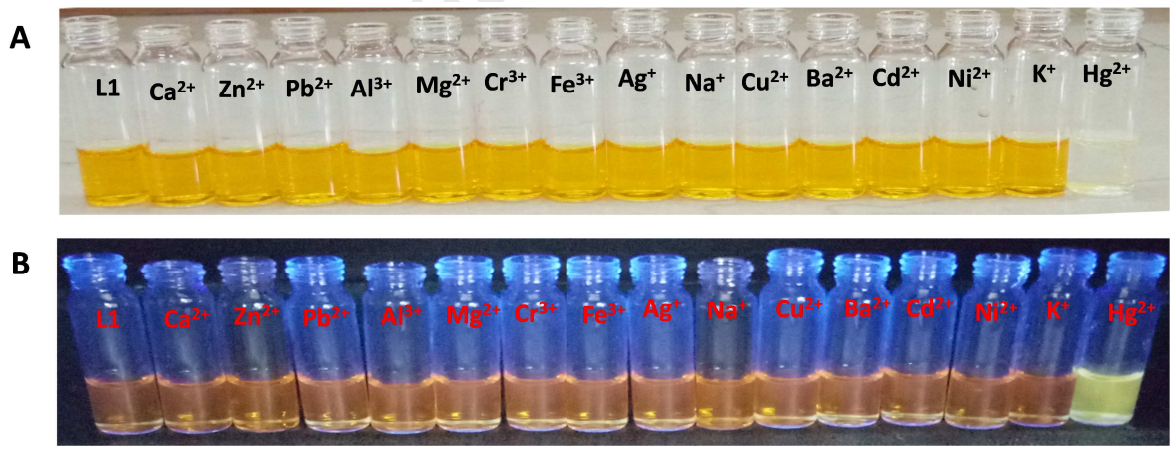

Figure 2 Free **L1** and **L1** in presence of different metal ions in aqueous medium (A) photograph in daylight and (B) photograph under UV light (365 nm).

UV–Vis spectral characteristics of L1 with metal ions

In order to investigate the selective recognition and binding of metal ions and to study the binding mechanism, the UV-Vis absorption characteristics of the chemosensor **L1** was studied in presence of different metal ions such as Ca^{2+}, Zn^{2+}, Pb^{2+}, Al^{3+}, Mg^{2+}, Cr^{3+}, Ba^{2+},

Cd^{2+}, Na^{+}, Cu^{2+}, Ni^{2+}, K^{+}, Ag^{+} and $Fe3^{+}$ (as their nitrate salts) in aqueous as well as in MeOH-H_2O (4:1 v/v) mixture. The aqueous solutions of different metal ions were added separately to the prepared solution of compound **L1** and UV-Vis absorption spectra were recorded. Upon addition of Hg^{2+} solution to the aqueous solution and also to MeOH-H_2O (4:1 v/v) of **L1**, the ICT band suffered hypochromicity and a new absorption band appeared at ~355 nm (Figure 3) However, no significant change in the absorption spectrum was observed in presence of other tested metal ions. The observed change in the UV-Vis spectral characteristics on addition of Hg^{2+} was found to be greater in methanol-water mixture, as compared to pure aqueous medium. This may be attributed to greater and stronger binding of metal ion with the host molecule in methanol-water medium. In contrary, in aqueous solution, a smaller and weaker binding of metal ion is anticipated due to greater and stronger solvation of Hg^{2+} ion in pure water which may restrict the interaction with the host molecule.

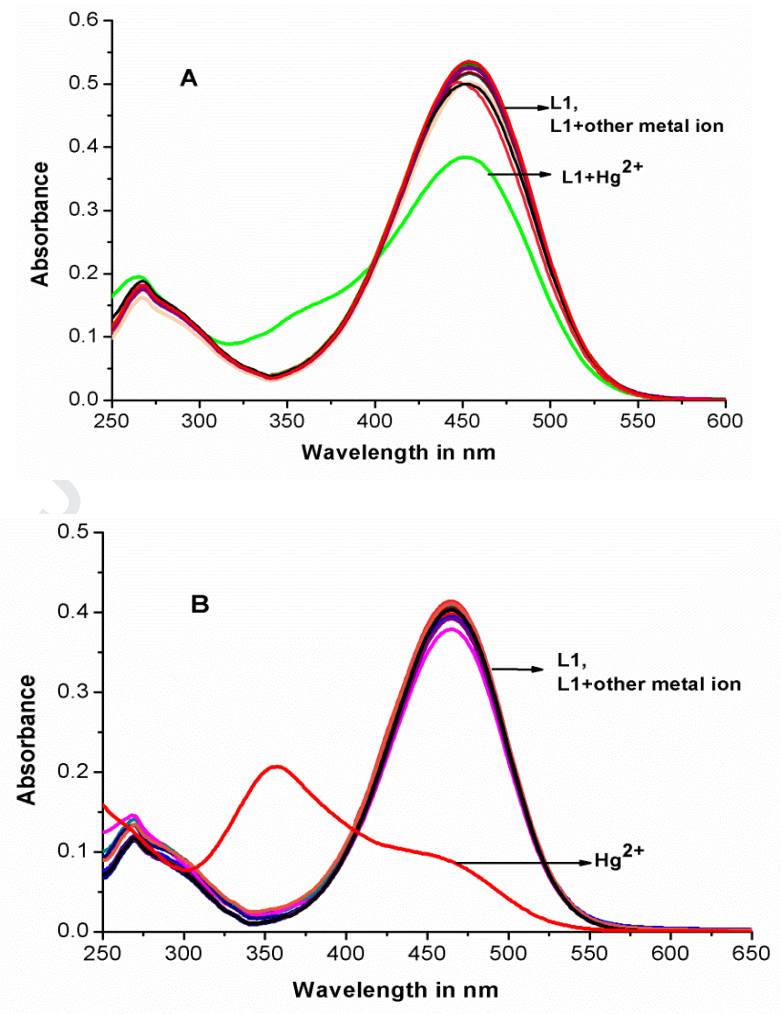

Figure 3 UV-Vis absorption band of the probe **L1** (12 μM) in presence of different metal ions (48 μM) in (A) H_2O medium (B) methanol-H_2O (4:1 v/v) medium.

To gain insight into the specific interaction with Hg^{2+} ion, UV-vis absorption titration of the chemosensor **L1** (12 μM) was performed with gradual increase in the concentration of Hg^{2+} (0-108 μM) ion. The UV-Vis absorption spectrum of free chemosensor L1 was found to be perturbed drastically. With increase in Hg^{2+} concentration (0-108 μM), absorbance of the ICT band centered at 455 nm started decreasing with concomitant increase in the absorbance of the newly developed absorption band at lower wavelength centered ~355 nm (Figure 4). The new absorption band was thus attributed to L1-Hg^{2+} bound species. Appearance of three well defined isosbestic points *ca*. 390, 300 and 258 nm clearly demonstrated the interconversion from free un-complexed species (**L1**) to complexed bound species (L1-Hg^{2+}). The decrease in the absorbance of ICT band clearly showed the involvement of the tertiary N-donor atom for the binding of Hg^{2+} ion. Upon binding with the metal, N-donor atom may acquire partial positive charge resulting in inhibition of intramolecular charge transfer in the D-π-A chromophore **L1**.

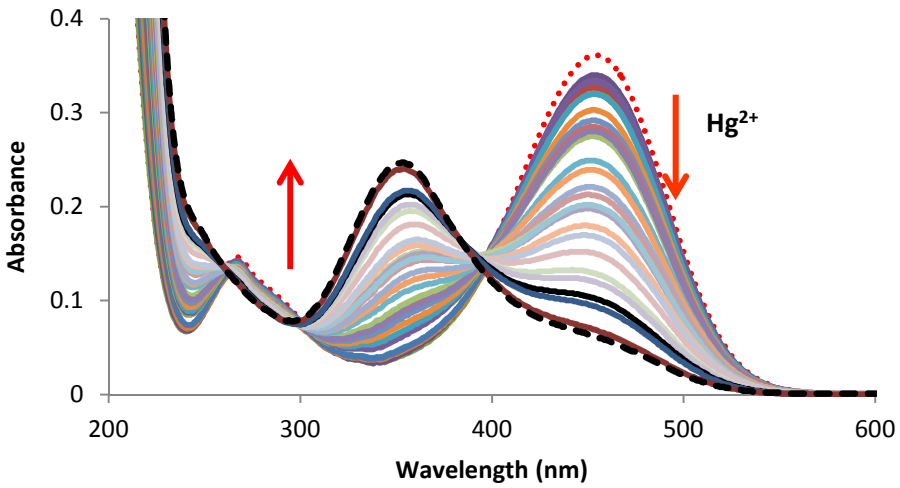

Figure 4 Changes in the UV-Vis absorption spectra of **L1** (12 μM) upon addition of increasing amount of Hg^{2+} ion (0-108 μM) in H_2O medium.

Fluorescence spectral characteristics of L1 with metal ions

Similar to UV-Vis absorption studies, fluorescence emission experiments were also carried out for free **L1** and metal bound species in methanol-H_2O (4:1 v/v) medium. Fluorescence spectra of the chemosensor **L1** at an excitation wavelength of 360 nm in the absence and presence of different metal ions such as Ca^{2+}, Zn^{2+}, Pb^{2+}, Al^{3+}, Mg^{2+}, Cr^{3+}, Ba^{2+}, Cd^{2+}, Na^{+}, Cu^{2+}, Ni^{2+}, K^{+}, Fe^{3+}, Ag^{+} (as their nitrate salts) have been collected and represented in Figure 5.

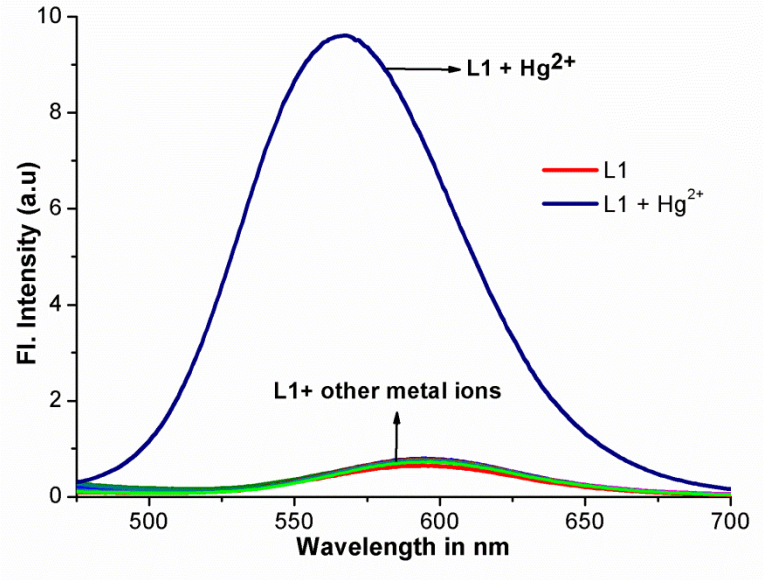

Figure 5 Fluorescence emission spectra of **L1** (12 μM) in presence of different metal ions (48 μM) in methanol-H_2O (4:1 v/v) medium (λ_{ex} = 360 nm)

The chemosensor L1 in its free state was found to be weakly fluorescent (quantum yield (ϕ_f) = 0.009) giving a low intense broad emission band at *ca.* 590 nm. Upon treating with 4 equivalents of different metal ions separately, except in the case of Hg^{2+} ion no significant change in the fluorescence spectrum was observed (Figure 5). On adding Hg^{2+} ion, remarkable enhancement was observed in the fluorescence intensity (ϕ_f = 0.044) with a blue shift of the emission wavelength to 566 nm. This turn-on fluorescence response may be explained through the following two factors. (i) Principle of chelation enhanced fluorescence (CHEF) as a consequence of inhibition of photo induced electron transfer (PET)[6,13, 31-33] and (ii) increase in conformational rigidity.[34-35]

Most of the turn-on chemical sensors are non-fluorescent or weakly fluorescent in their free state possibly due to PET (photo induced electron transfer) effect. The metal binding host unit of these sensors contain lone pair of electrons on the hetero-atoms (such as, nitrogen, oxygen, sulphur atoms or with any other functional groups), which are of higher energy than the highest occupied molecular orbital (HOMO) of the fluorophore. Upon excitation of an electron from the HOMO to the lowest unoccupied molecular orbital (LUMO) of the fluorophore, these lone pair of electrons jump down immediately to fill the partially empty HOMO of the fluorophore, which inhibits the excited electron to return back to the fluorophore ground state HOMO and there by quenching fluorescence (Scheme 2). Involvement of these lone pairs for metal chelation drops the energy of lone pair below that

of the fluorophore HOMO, consequently prevents the process of PET resulting in enhanced fluorescence (CHEF).[31-33] Similarly, in the present case binding of Hg^{2+} to the NS_2O_2 binding site of the chemosensor **L1** through the lone pairs on nitrogen, oxygen and sulphur make them unavailable for any possible PET effect, which may result in strong fluorescence enhancement.

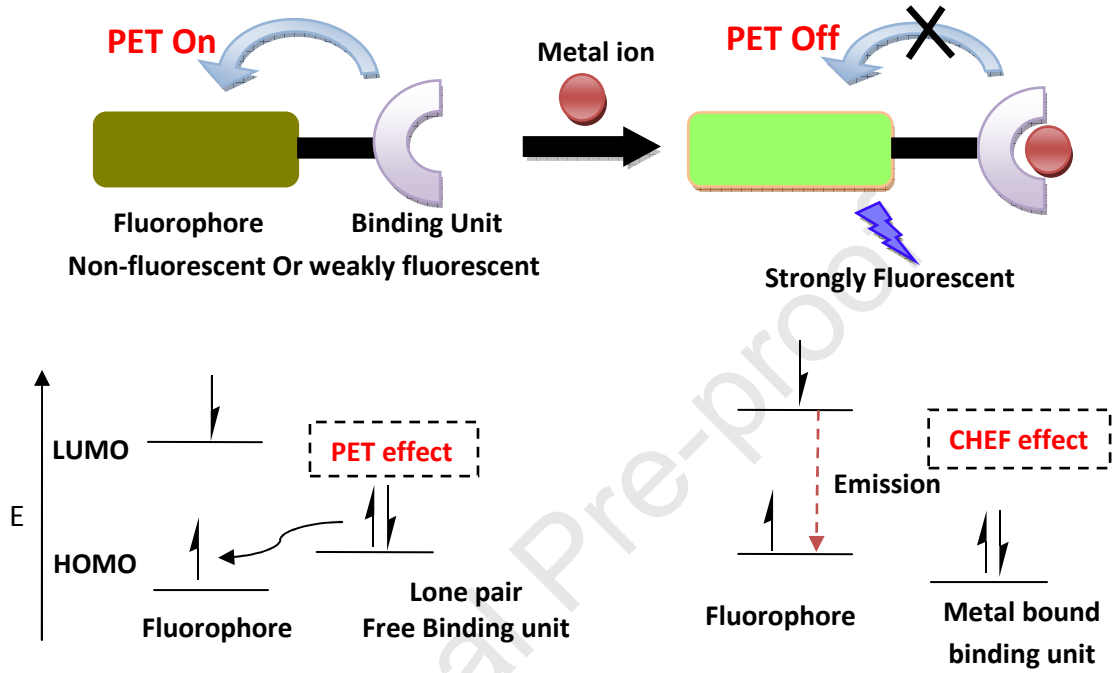

Scheme 2 Schematic representation of fluorescence quenching by PET effect and fluorescence enhancement by CHEF effect.[31-33]

Fluorescence intensity is often related to the rigidity of the chromophore structure. In general, the restricted rotational motion of the fluorophore makes the rotation-related nonradiative decay pathway less efficient, hence enhancing the fluorescence quantum yield and intensity.[34-35] The strong enhancement of fluorescence intensity of **L1** in its mercury bound state may also be attributed to the restriction of the torsional motion of disubstituted amino group imposed by the formation of L1-Hg^{2+}complex making it conformationally more rigid than the unbound **L1** which possibly resulting in increased fluorescence intensity through a reduction of non-radiative decay. In order to confirm this proposition, the fluorescence lifetime studies were carried out for free **L1** and L1-Hg^{2+}complex in methanol-H_2O (4:1 v/v) medium. The unbound ligand exhibited tri-exponential fluorescence decay with an average fluorescence lifetime of 0.25 ns, which increased to 0.56 ns in presence of mercury ion. From the average fluorescence lifetime and quantum yield values the radiative

(k_f) and non-radiative (k_{nr}) decay constants were computed and the values are represented in Table 1. As evident from the data, there is a significant reduction in the k_{nr} value in presence of mercury thus supporting the above proposition *i.e.* formation of L1-Hg^{2+}complex induces a conformational rigidity in the fluorophore. As as a consequence there is a reduction in non-radiative decay, which in turn results in an enhanced fluorescence quantum yield.

Table 1 Comparison of average fluorescence lifetime, quantum yield, radiative (k_f) and non-radiative (k_{nr}) decay constants for **L1** and L1-Hg^{2+} complex in MeOH:H_2O(4:1) medium

System	τ_1 (ns)	α_1 (%)	τ_2 (ns)	α_2 (%)	τ_3 (ns)	α_3 (%)	τ_{avg} (ns)	Φ_f	k_f (ns^{-1})	k_{nr} (ns^{-1})
L1	0.14	90.33	0.71	8.31	4.5	1.35	0.25	0.009	0.037	4.025
L1+Hg	0.35	46.34	0.74	53.66	--	--	0.56	0.044	0.079	1.709

Remarkable increase in fluorescence intensity, quantum yield and lifetime along with a blue shift of *ca.* 26 nm in presence of Hg^{2+} is thus a result of the binding of donor group with the metal ion, restriction in bond rotation by giving a rigid environment and inhibition of PET induced quenching in the L1-Hg^{2+} adduct. The selective fluorescence enhancement could be due to more effective and strong binding of Hg^{2+} with the donor atoms of **L1** in comparison with other metal ions. However, a detailed analysis of the photo-physics of the fluorophore with and without metal ion is essential for a definite conclusion.

Selectivity and non-interference of L1

In order to establish the high selective nature of chemosensor **L1** towards Hg^{2+}, the effect of other metal ions on the fluorescence emission was investigated. The interference experiments were conducted by adding excess of the interfering metal ion (240 μM) namely Ca^{2+}, Zn^{2+}, Pb^{2+}, Al^{3+}, Mg^{2+}, Cr^{3+}, Ba^{2+}, Cd^{2+}, Na^{+}, Cu^{2+}, Ni^{2+}, K^{+}, Ag^{+} and Fe^{3+} to the solution of Hg^{2+} (48 μM) and the probe L1 (12 μM). The fluorescence intensities were analysed and plotted as a bar graph in Figure 6. No considerable change was observed in the fluorescence emission profiles of L1-Hg^{2+} solution, indicating that the probe has a strong selective binding ability for Hg^{2+} even in presence of different interfering metal ions encountered in environmental and biological samples.

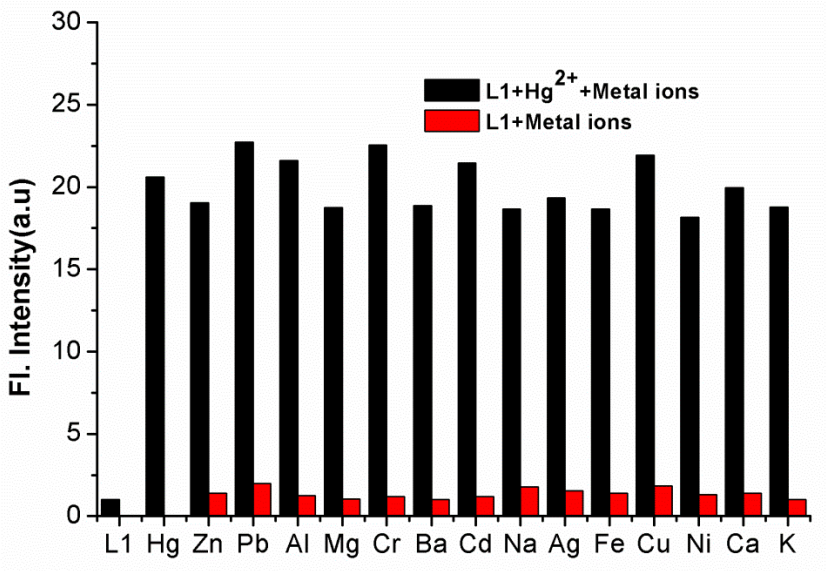

Figure 6 Bar graph of fluorescence intensity (at 566 nm) for the solution of free L1 (12 μM), L1 with Hg^{2+} (48 μM), L1 with Hg^{2+} (48 μM) in the presence of other competitive metal ions (240μM) in MeOH:H_2O(4:1) medium. The red bars and black bars represent the fluorescence intensity of solution of **L1** in the presence of 48 μM of other tested metal ions in the absence of Hg^{2+} and in presence of Hg^{2+} ion respectively. (λ_{ex} = 360 nm)

Binding stoichiometry, association constant and limit of detection (LOD)

The binding stoichiometry of the probe **L1** with Hg^{2+} ion was quantified by Jobs's method. For this the emission spectral data were collected at a constant total molar concentration of 12μM with continuous variation of mole fraction of the two binding species (Figure 7a). Figure 7b represents the change in fluorescence intensity with change in mole fraction of Hg^{2+}. A maximum at a mole fraction of 0.5 clearly established the formation of a 1:1 binding of the probe with the metal ion to form L1-Hg^{2+} complex in methanol-H_2O (4:1 v/v) medium.[36]

The association constant (K) for the binding of the probe with Hg^{2+} was determined from fluorescence spectral emission data in water medium as well as in MeOH-H_2O (4:1 v/v) medium using Benesi-Hildebrand equation (equation 1).[37]

$$\frac{1}{I-I_0} = \frac{1}{I_{max}-I_0} + \frac{1}{K(I_{max}-I_0)[Hg^{2+}]} \qquad (1)$$

Where I_0, I_{max}, and I refers to fluorescence intensity of free L1 in the absence of Hg^{2+}, maximum fluoresce intensity in presence of Hg^{2+} at a concentration of complete interaction and intermediate fluoresce intensity at varying [Hg^{2+}].

Using slope and intercept of the plot of $1/(I-I_0)$ versus $1/[Hg^{2+}]$, K was calculated to be 1.13 x 10^5 M^{-1} and 1.46 x 10^5 M^{-1} in water and in MeOH-H_2O (4:1 v/v) medium respectively (Figure 8 A and B). The lower value of association constant in water medium compared to that of methanol-water mixture is probably due to greater solvation of Hg^{2+} ion in water which may restrict the interaction of L1 and metal ion.

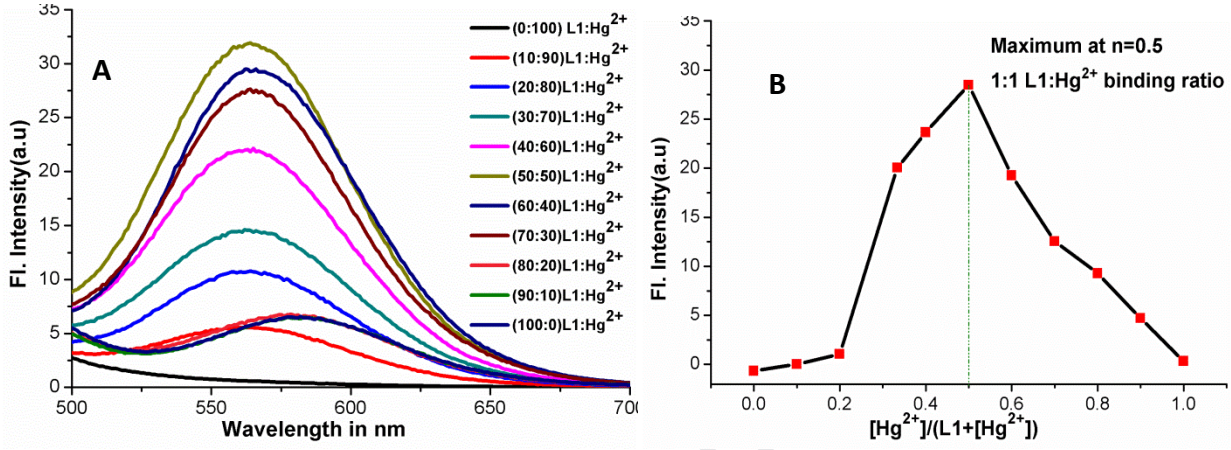

Figure 7 (A) Fluorescence spectra of solution containing L1 and Hg^{2+} with varying molef fraction at a total molar concentration of 12μM and (B) respective Job's plot of Hg^{2+} mole fraction vs. fluorescence intensity at 566 nm (λ_{ex} = 360 nm).

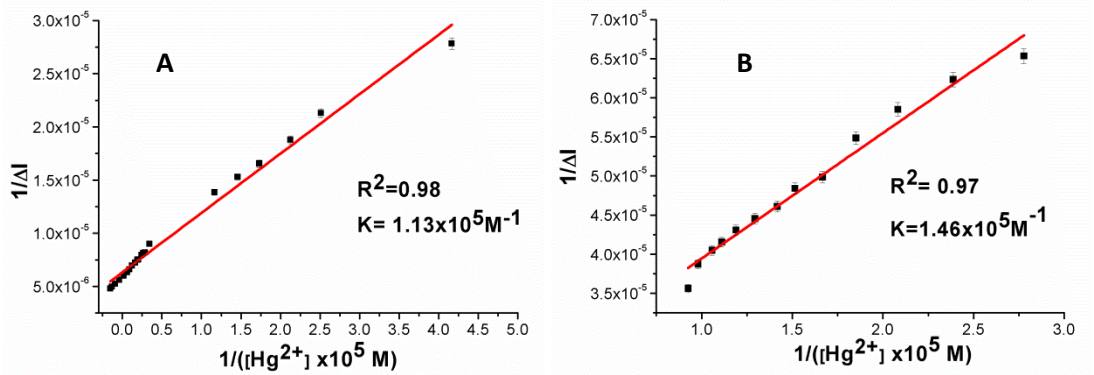

Figure 8 Plots of $1/(I-I_0)$ versus $1/[Hg^{2+}]$ in (A) water medium (B) in MeOH-H_2O (4:1 v/v) medium.

In order to perform as a suitable chemosensor one of the major concern is the sensitivity or limit of detection (LOD) of the probe. To determine the sensitivity of the probe **L1**, a fluorescence titration experiment in water medium was performed with increasing $[Hg^{2+}]$ (0-30 μM) at constant **[L1]** (12 μM) (Figure 9A) On addition of Hg^{2+} up to a concentration of 3.6μM no significant change was observed. However, when the $[Hg^{2+}]$ is ≥ 4.8μM, detectable enhancement in fluorescence intensity with gradual blue shift of the peak was observed. This experiment demonstrated a low detection limit (DL) of **L1** towards Hg^{2+}

i.e. 4.8 µM. Further, LOD was also calculated using the extensively used method *i.e.* LOD = 3σ/S, where σ is the standard deviation intercept and S is the slope of the linear fitting equation of the plot I/I_0 versus [Hg^{2+}] (Figure 9B). LOD calculated using this method was found to be 7.5 µM. DL and LOD for the present work is comparable with that of previously reported literature (Table 2). [38-43]

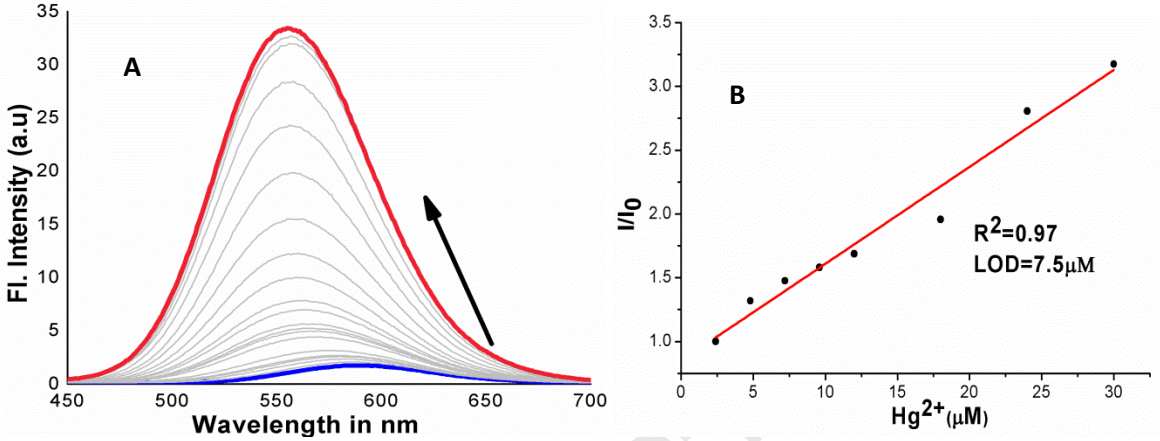

Figure 9 (A) fluorescence titration experiment with increasing [Hg^{2+}] (0-48 µM) at constant **[L1]** (12 µM) in water medium, (B) linear plot of (I/I_0) versus [Hg^{2+}].

Table 2 Comparison of LOD for Hg^{2+} of the present chemosensor with previously reported literatures.

References	Fluorophore/Chromophore	Type of detection	Solvent medium	LOD
Ref 38	Pyrazidine derivative	Colorimetric and fluorescence	Water	14.54µM
Ref 39	HOE DNA binding dye	fluorescence	Water	0.87µM
Ref 40	Thiophene-based Schiff base	Colorimetric and fluorescence	MeOH:H_2O	20µM
Ref 41	Rhodamine B/ Spirolactam ring	Colorimetric and fluorescence	Water	10µM
Ref 42	Rhodamine derivative	fluorescence	MeOH:H_2O	10µM
Ref 43	BODIPY	fluorescence	Water	4.2µM
This work	Styryl pyridinium dye	Colorimetric and fluorescence	Water	7.5µM

Nature of binding Interaction: ^{1}H NMR spectroscopic analysis

In order to confirm the binding mode of the compound **L1** with Hg^{2+} ion, ^{1}H-NMR spectroscopic studies were carried out. The ^{1}H-NMR spectra of the chemosensor **L1** before and after treatment of Hg^{2+} in DMSO-d_6 are presented in Figure 10. All the ^{1}H-NMR peaks of **L1** are found to be downfielded to more or less extent after addition of mercury. However significant change in the proton signal for H1, H2, H3, H4, H5 H6 and H9 are observed as follows. (i) Peak for the -OH proton (H1) at δ 4.83 ppm disappeared on addition of Hg^{2+} probably because of binding of oxygen atom to metal ion which may weaken the O-H bond leading to deprotonation. (ii) Proton signal for $–CH_2$ proton attached to O atom (H2) and N atom (H5) appeared as multiplet at δ 3.53 ppm are found to be slightly downfielded, separated progressively with increasing concentration of Hg^{2+} and appeared as two distinct triplets at δ 3.56 and δ 3.7 ppm respectively. (iii) Peak for $–CH_2$ proton attached to S atom (H3 and H4) appeared as two distinct triplets at δ 2.62 ppm and δ 2.69 ppm respectively in free **L1** are found to be downfielded and merged with gradual addition of Hg^{2+} to give a distorted broad triplet at δ 3.15 ppm. This may be because of decrease in electron density at S atom due to strong covalent type binding interaction with mercury ion. (iv) Doublet for H6 *i.e. ortho* to the electron donating N-atom at δ 6.73 ppm is also downfielded to a great extent and appeared at δ 7.16 ppm which may be due to decrease in electron density on N-atom upon association with the metal ion. Thus the change in ^{1}H NMR chemical shifts demonstrated a clear picture of an adduct formation between the sensor **L1** with metal cation chelated through N, S and O donor atom.

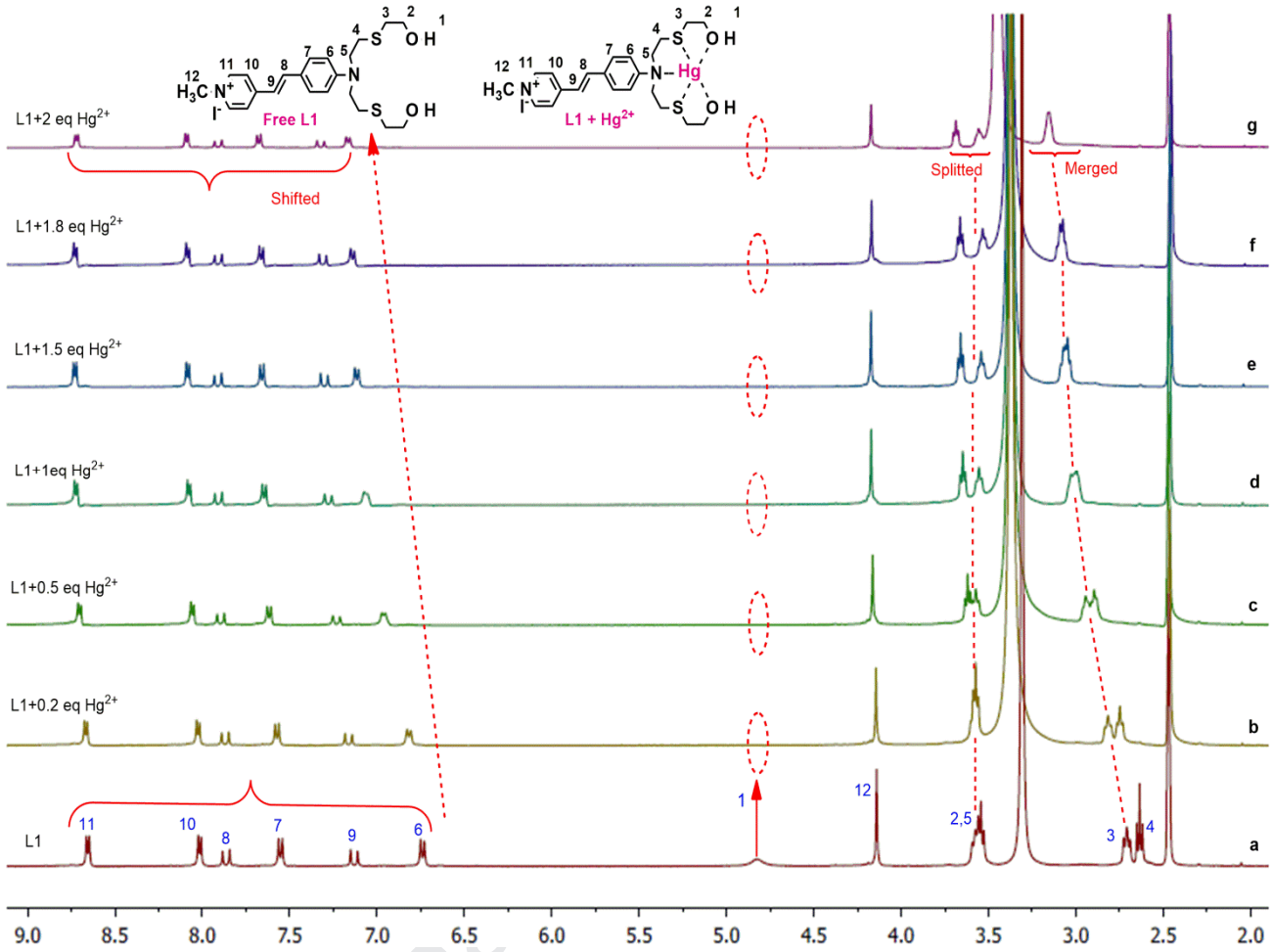

Figure 10 ^{1}H-NMR spectra of probe **L1** and L1+ Hg^{2+} in DMSO-d_6 and a possible mode of binding interaction (a) Free L1 (b) L1 + 0.2 eq. Hg^{2+} (c) L1 + 0.5 eq. Hg^{2+} (d) L1 + 1 eq. Hg^{2+} (e) L1 + 1.5 eq. Hg^{2+} (f) L1 + 1.8 eq. Hg^{2+} (g) L1 + 2 eq. Hg^{2+}

FESEM analysis

Cyanine dyes can spontaneously self assemble to form aggregates *via* intermolecular van der Waals forces. By varying solvent or adding salt, the aggregates can be transformed into various forms, for example, H- or J-aggregates, which can be easily distinguished by different analytical techniques.[44] To observe any morphological alteration of chemosensor L1 after chelation to Hg^{2+}, FESEM analysis was attempted. Whereas the neat styryl dye **L1** possessed wire like microstructure which was found to be disrupted to a flower like morphology upon treatment with Hg^{2+} (Figure 11A & B). The reorganization of the aggregated probe **L1** might be attributed to the formation of L1-Hg^{2+} adduct. The chemical composition of the L1+Hg^{2+} complex was also measured by the EDAX analysis which clearly showed the presence of

carbon (C), oxygen (O), nitrogen (N), sulphur (S) and mercury (Hg) in the prepared L1+ Hg^{2+} complex (Figure 11D).

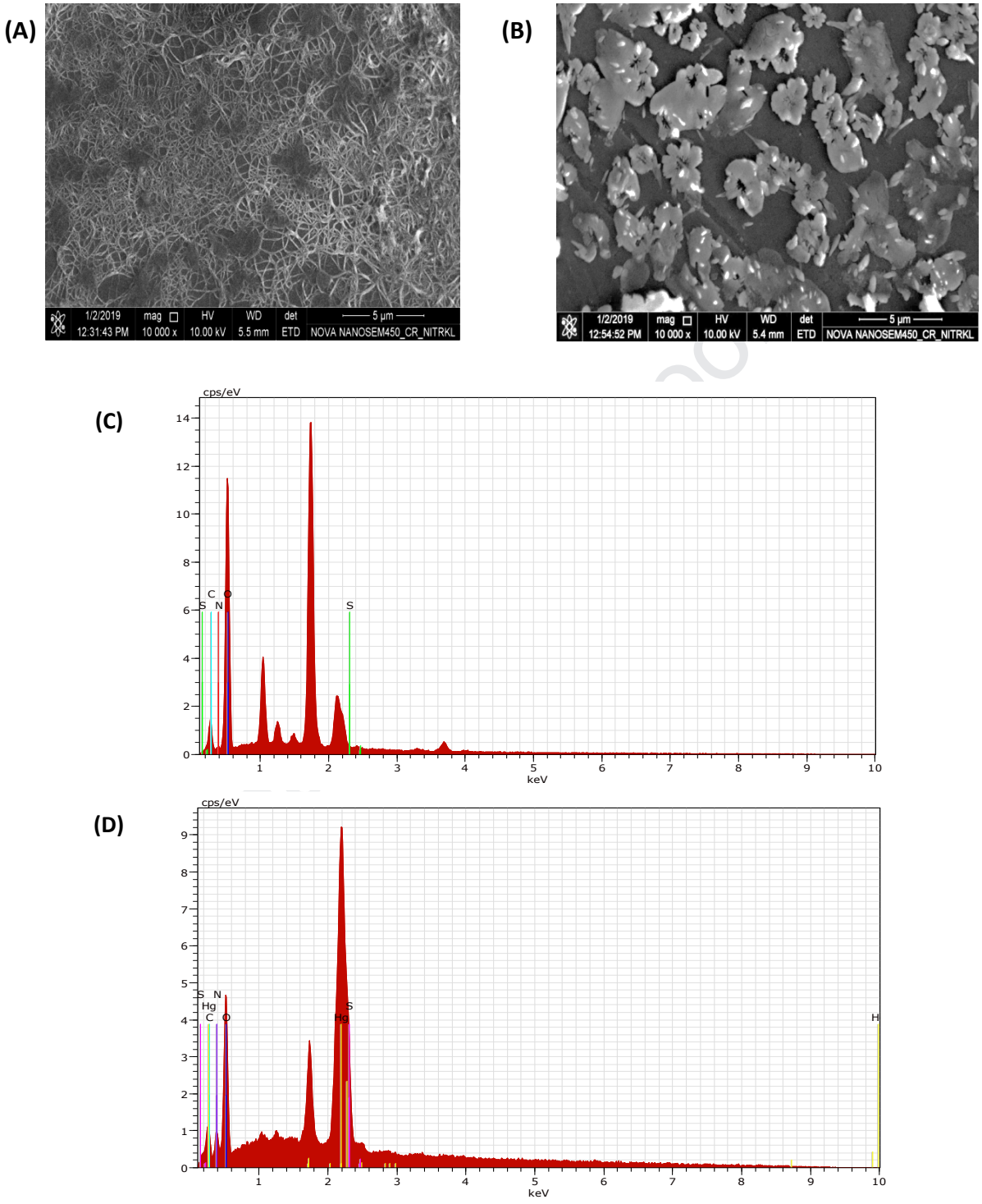

Figure 11 SEM images of (A) Free L1 (B) L1 + Hg^{2+} (C) EDX pattern of L1 (D) EDX pattern of L1 + Hg^{2+} adduct.

*Reversibility of the chemosensor **L1***

The reversible binding behaviour of chemosensors towards specific analytes is a vital aspect for practical application. The reversibility of the chemosensor **L1** was tested with sodium sulphide (Na_2S). Addition of Na_2S (24 µM) to the solution containing L1(12µM) and Hg^{2+} (48µM) resulted in a dramatic quenching of the fluorescence emission intensity (Figure 12). The colour of the solution as well as fluorescence intensity at 566 nm was found to revert back to that of free **L1** solution. It may be explained through strong affinity of sulphide anion (S^{2-}) for the Hg^{2+} cation, causing demetallation of the L1-Hg^{2+} complex with a simultaneous decrease in the fluoresce intensity due to non-availability of Hg^{2+} for chelation. After the addition of 1 equiv. (12 µM) of Hg^{2+} again to the same solution, the fluorescence of the solution was revived. Furthermore, upon the sequential alternate addition of S^{2-} and Hg^{2+} into the solution, the fluorescence switching response could be repeated for several cycles. These results suggested that L1 can be used as a reversible fluorescent chemosensor for the selective detection of Hg^{2+} ions in aqueous as well as in aqueous-alcoholic mixtures under physiological conditions.

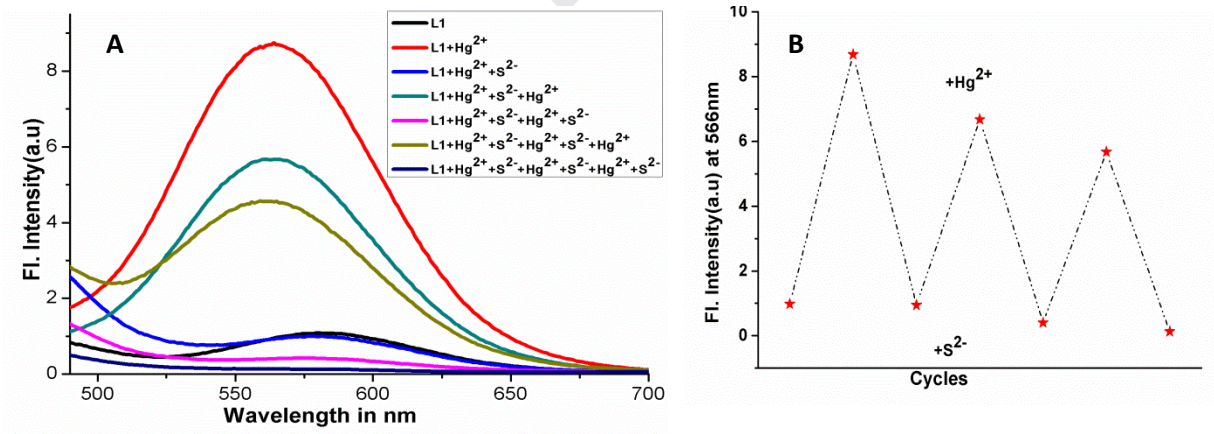

Figure 12 The reversible binding behaviour of **L1** with Hg^{2+} tested using S^{2-} anion.(A) Emission spectra and (B) Emission intensity (at 566nm) of L1 with sequential addition of Hg^{2+} and S^{2-}.

Construction of Logic Gate

The clear "off–on" fluorescence response of the chemosensors in response to the addition of metal shows the digital action of molecules and thus applied to combinational logic circuit.[45] The reversible binding behaviour of chemosensor L1 to Hg^{2+} and consequent changes in fluorescence intensity at 566 nm in presence and absence of S^{2-} mimics the INHIBIT logic gate.[46] Figure 13 demonstrated the circuits for the INHIBIT logic gate. This was constructed with Hg^{2+} (Input 1)

and S^{2-} (Input 2) as two chemical inputs and the fluorescence intensity at 566 nm as output. The presence of Hg^{2+} and S^{2-} was defined as binary "1", and the absence of these inputs was defined as binary "0" (Table 2). For the output, the value of I/I_0 at 566 nm was considered as "1" for strong enhanced fluorescence (turn-on) and "0" for weak quenched fluorescence (turn-off). As shown in Figure 14, when input of Hg^{2+} (Input 1) was present alone, output "1" was obtained because the L1 solution showed a prominent turn-on fluorescence response at 566 nm. In other input combinations, the output signal was "0", implying turn-off fluorescence. The behaviour is properly fitting with INHIBIT logic gate. This molecular switching behaviour might be applied to the development of smarter fluorescent material for multitasking biosensing applications.

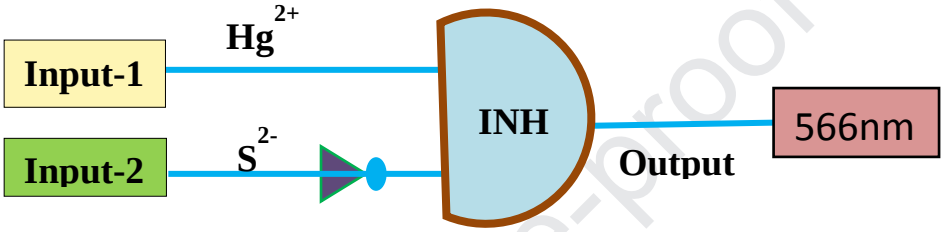

Figure 13 The circuit diagram for the INHIBIT logic gate

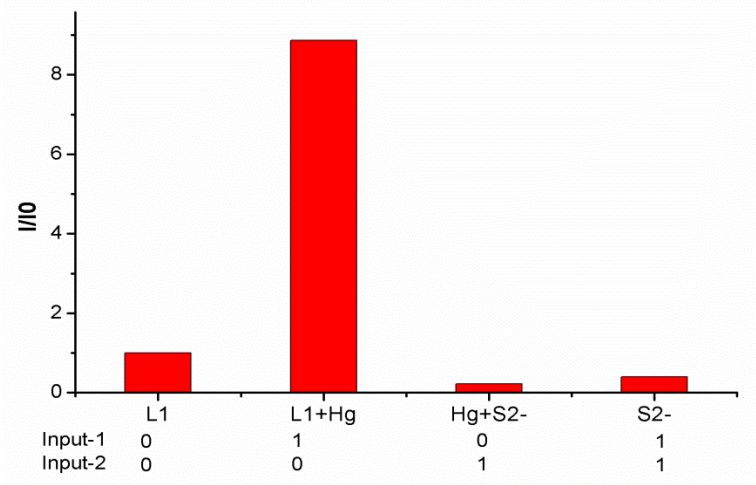

Input 1 (Hg^{2+})	Input 2 (S^{2-})	Output (λ=566nm)
0	0	0
1	0	1
0	1	0
1	1	0

Figure 14 The fluorescence intensity of L1 at 566 nm in the presence of four different inputs and truth table for the INHIBIT logic gate

Based on the above collective results from UV-Vis absorption, Fluorescence emission, Job's plot analysis, NMR interpretation and reversibility test, the selective 1:1 binding of probe **L1** with Hg^{2+} ion and the probable mechanism of turn-on fluorescence enhancement is schematically represented below (Scheme 4). The chemosensor **L1** in its free form has a visible absorption due to ICT transition, gives an orange colour in water medium and is weakly fluorescent for possible electron transfer upon photo excitation (PET). Owing

to the involvement of donor tertiary amino N atom in the metal bound form, while it becomes colourless as a result of absence of ICT, absence of PET and increased rigidity due to chelation produce a large enhancement in fluorescence intensity (CHEF).

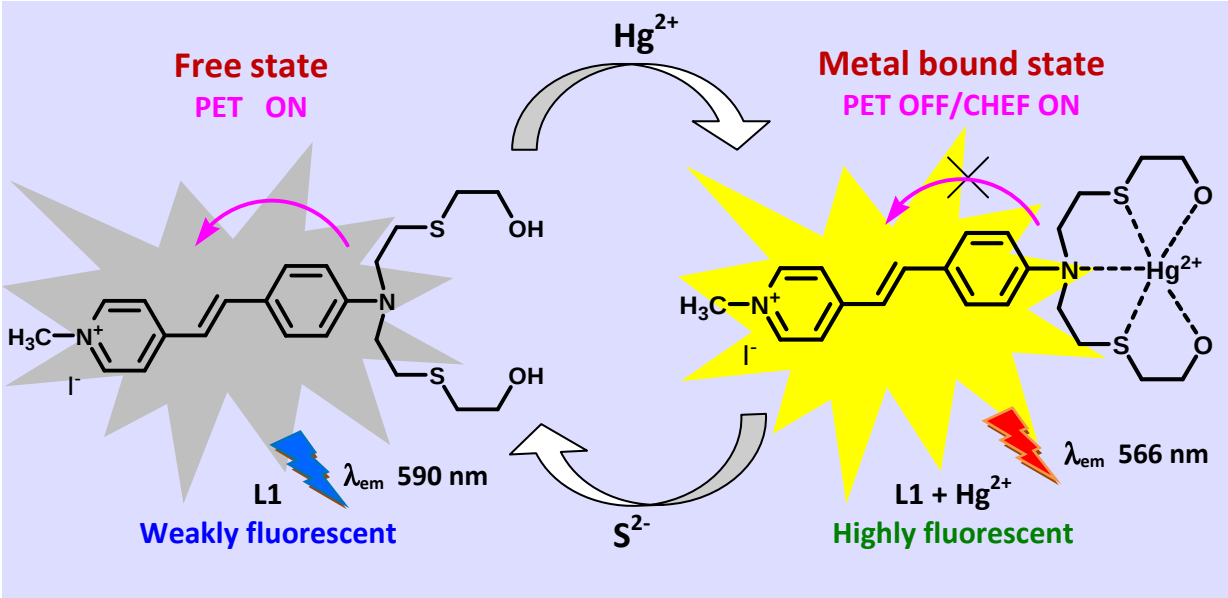

Scheme 4 Proposed binding mode of the chemosensor **L1** with Hg^{2+} and probable mechanism of turn-on sensing.

Application of chemosensor L1 in cell imaging

Among numerous potential applications of cyanine dyes, bioimaging as fluorescence probes in living cells has attracted a great deal of attention recently.[47] Zhou *et al.* reported that cyanine chromophore could interact with DNA in the mode of intercalation and be effectively used as fluorescent staining dye for cell imaging applications. They have also reported the non-toxic nature of the chromophore by examining cell viability data for MCF-7 (Human breast carcinoma) cells at micromolar concentrations and can applied in brighter twophoton fluorescent (TPF) bioimaging.[48] In the present work, for practical applicability of sensor **L1**, permeability and detection of Hg^{2+} within living bacterial cell in an image wise manner was explored. For this, the E.coli DH5-α bacterial cells were grown overnight in LB (Luria Bertani) medium at 37 ^{O}C in a shaker incubator. These bacterial cells were further incubated with 48 μM of $Hg(NO_3)_2$ in PBS (phosphate buffered saline) buffer at 37 °C for 2 h. To remove the remaining $Hg(NO_3)_2$, the bacterial cells were washed with PBS buffer and incubated further with 12 μM of sensor **L1** in Methanol:PBS for half an hour at room temperature. After washing again with PBS, these bacterial cells were transferred to glass slide for imaging. Fluorescence images of bacterial cells were gleaned using a Leica TCS

SP8 confocal laser scanning microscope attached to a Leica DMi8 inverted epifluorescence microscope. Figure 16 displayed the fluorescence images of bacteria cell in the absence and presence of Hg^{2+} and probe **L1**. This test indicated that the bacterial cell emits red fluorescence with **L1** in presence of Hg^{2+} under fluorescence microscope. It revealed that the probe **L1** has cell membrane permeability for cell imaging and thus can be utilised for intracellular detection of Hg^{2+} in living cells.

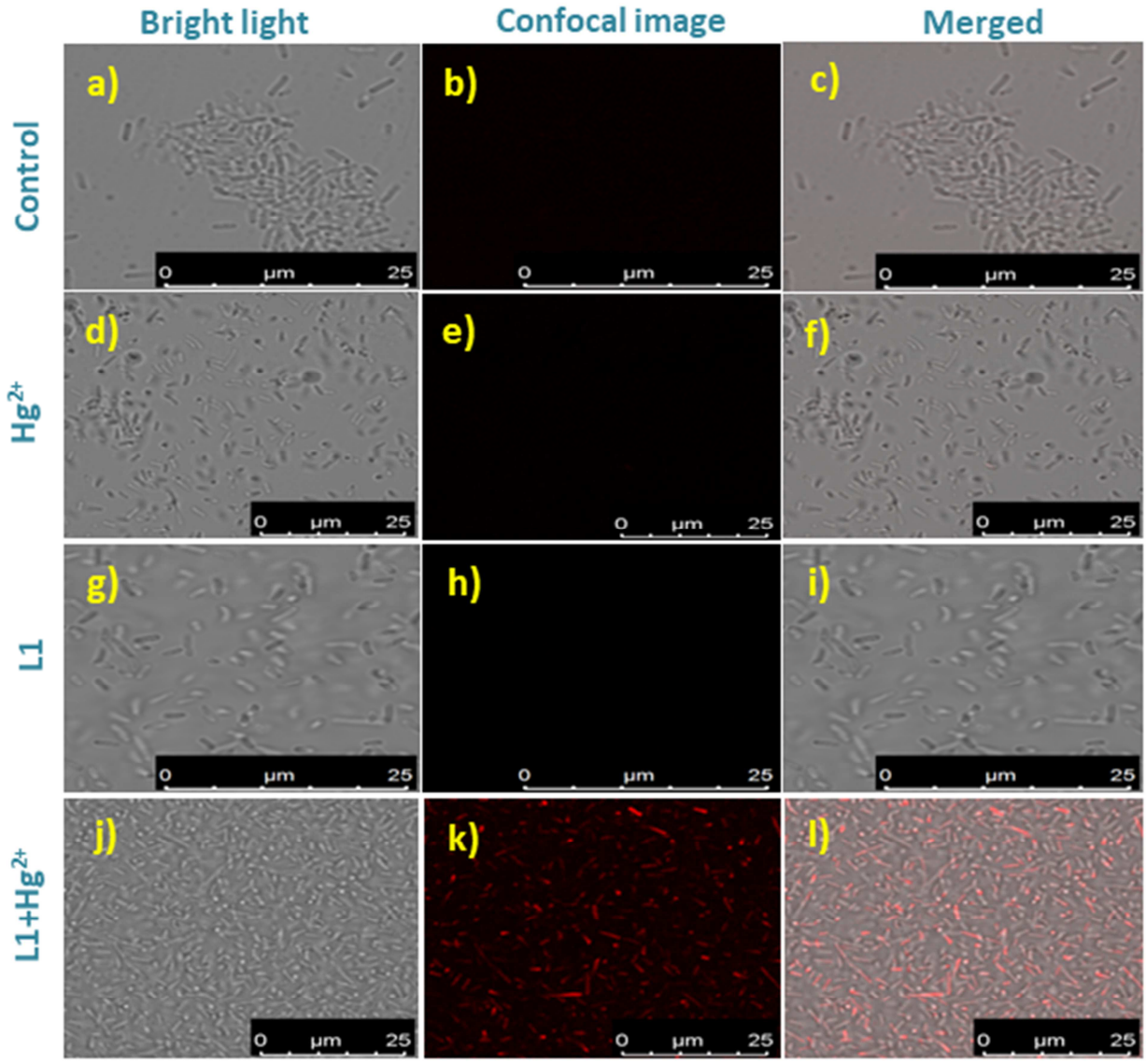

Figure 16 Confocal fluorescence images: (a) bright field image (b) confocal image (c) a merged of (a) and (b) of E.coli DH5-α cells; (d) bright field image (e) confocal image of (f) a merged of (d) and (e) of E.coli DH5-α cells stained to Hg^{2+} (48 µM); (g) bright field image (h) confocal image (i) a merged image of (g) and (h) of E.coli DH5-α cells stained to **L1** (12 µM); (j) bright field image (k) confocal image (l) a merged image of (j) and (k) of E.coli DH5-α cells stained to **L1** (12 µM) and Hg^{2+} (48 µM).

*Application of chemosensor **L1** in test paper strips*

Based on the differential colour of L1 in its free form and in Hg^{2+} bound form, it can be used as a useful means for naked eye detection of Hg^{2+} in aqueous and aqueous-organic media. Further for practical usage and for easy detection of mercury content, paper strip method was applied. For this paper strip made up of whatman filter paper were prepared by treating the paper with a solution of **L1** (0.3 mM) in methanol and dried with air. The test paper strip was then immersed in an aqueous solution of Mercuric nitrate (1.2 mM) for 2 minutes and dried in air. Figure 17 shows the change in colour of paper strips with and without Hg^{2+} ions in day light and under UV light at 365 nm. The clear change in colour of the **L1** loaded test strip upon dipping in Hg^{2+} solution demonstrated the practical applicability for successful detection of Hg^{2+} metal ion on a solid paper strip.[49-50]

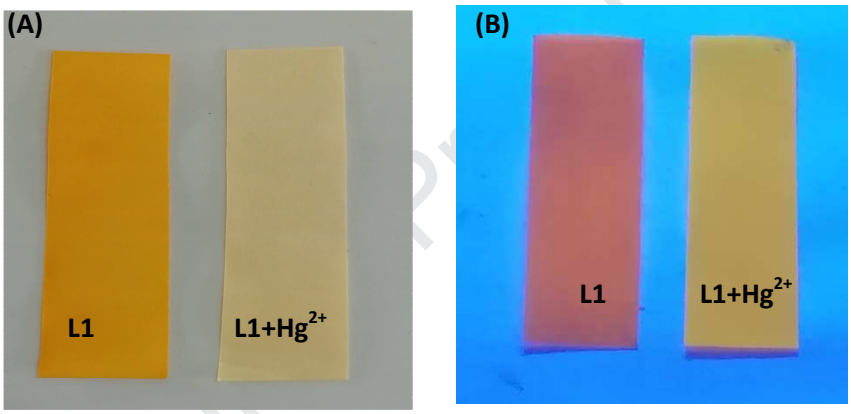

Figure 17 Photographs showing the colour change of probe L1 before and after addition of Hg^{2+} (A) in day light and (B) under UV light at 365 nm.

4. Conclusion

In conclusion, we demonstrate a simple and selective chromogenic and fluorogenic turn-on chemosensor based on a styrylpyridinium chromophore (L1) to detect Hg^{2+} ion in aqueous, aqueous-organic medium and in biological systems. The change in color of the solution from orange to colourless upon addition of Hg^{2+} ion is clearly visible to the naked eye. Significant increase in emission intensity of L1 upon interaction with Hg^{2+} is ascribed to CHEF due to the formation of a conformationally rigid stable L1 + Hg^{2+} adduct. Based on the collective experimental results from UV-Vis, fluorescence emission, Job's plot analysis, NMR interpretation and reversibility test, a selective and strong 1:1 binding of probe L1 with Hg^{2+} ion through the NS_2O_2 donor atoms is proposed. The molecular recognition with fluorescence

signal is used to construct an INHIBIT molecular logic gate based on the input/output characteristics of this molecular device. Moreover, chemosensor **L1** can be utilised to track the presence of Hg^{2+} ion in real-time in aqueous medium using naked-eye paper test strip method and in living cell by fluorescence imaging.

Conflicts of interest

The authors declare no competing financial interest.

Acknowledgements

SP gratefully acknowledge DST, New Delhi (SR/FT/CS-023/2009) and BRNS, Mumbai (37(2)/14/15/2018-BRNS) for financial support through research projects. Authors are grateful to Sambalpur University, Odisha, India for fluorescence lifetime measurement and NISER, Bhubaneswar, India for HRMS measurement.

5. References

1. X. Chen, T. Pradhan, F. Wang, J. S. Kim and J. Yoon, *Chem. Rev.*, 2012, **112**, 1910–1956.
2. X. Li, X. Gao, W. Shi and H. Ma, *Chem. Rev.*, 2014, **114**, 590–659.
3. R. Satapathy, Y. H. Wu and H. C. Lin, *Chem. Commun.*, 2012, **48**, 5668–5670.
4. C. Mcdonagh, C. S. Burke and B. D. Maccraith, *City*, 2008, **108**, 400–422.
5. X. Mao, H. Su, D. Tian, H. Li and R. Yang, *ACS Appl. Mater. Interfaces*, 2013, **5**, 592–597.
6. K. P. Carter, A. M. Young and A. E. Palmer, *Chem. Rev.*, 2014, **114**, 4564–4601.
7. R. Martínez, A. Espinosa, A. Tárraga and P. Molina, *Tetrahedron*, 2008, **64**, 2184 - 2191.
8. R. Dwivedi, D. P. Singh, S. Singh, A. K. Singh, B. S. Chauhan, S. Srikrishna and V. P. Singh, *Org. Biomol. Chem.*, 2019, **17**, 7497–7506.
9. A. P. De Silva, H. Q. N. Gunaratne, T. Gunnlaugsson, A. J. M. Huxley, C. P. McCoy, J. T. Rademacher and T. E. Rice, *Chem. Rev.*, 1997, **97**, 1515–1566.
10. D. Wu, A. C. Sedgwick, T. Gunnlaugsson, E. U. Akkaya, J. Yoon and T. D. James, *Chem. Soc. Rev.*, 2017, **46**, 7105–7123.
11. K. H. Kim, E. Kabir and S. A. Jahan, *J. Hazard. Mater.*, 2016, **306**, 376–385.
12. M. Farina, J. B. T. Rocha and M. Aschner, *Life Sci.*, 2011, **89**, 555–563.
13. H. Lee, H. S. Lee, J. H. Reibenspies and R. D. Hancock, *Inorg. Chem.*, 2012, **51**,

10904–10915.

14. D. V. Berdnikova, N. I. Sosnin, O. A. Fedorova and H. Ihmels, *Org. Biomol. Chem.*, 2018, **16**, 545–554.
15. Y. J. Lu, Q. Deng, D. P. Hu, Z. Y. Wang, B. H. Huang, Z. Y. Du, Y. X. Fang, W. L. Wong, K. Zhang and C. F. Chow, *Chem. Commun.*, 2015, **51**, 15241–15244.
16. M. Matsui, K. Ooiwa, A. Okada, Y. Kubota, K. Funabiki and H. Sato, *Dye. Pigment.*, 2013, **99**, 916–923.
17. W. Sun, S. Guo, C. Hu, J. Fan and X. Peng, *Chem. Rev.*, 2016, **116**, 7768–7817.
18. M. Panigrahi, S. Dash, S. Patel and B. K. Mishra, *Tetrahedron*, 2012, **68**, 781–805.
19. S. Dash, M. Panigrahi, S. Baliyarsingh, P. K. Behera, S. Patel and B. K. Mishra, *Curr. Org. Chem.*, 2011, **15**, 2673–2689.
20. A. Mishra, R. K. Behera, P. K. Behera, B. K. Mishra and G. B. Behera, *Chem. Rev.*, 2000, **100**, 1973–2011.
21. J. L. Bricks, A. D. Kachkovskii, Y. L. Slominskii, A. O. Gerasov and S. V. Popov, *Dye. Pigment.*, 2015, **121**, 238–255.
22. H. Zheng, M. Yan, X. Fan, D. Sun, S. Yang and L. Yang, *Chem. Commun.*, 2012, **48**, 2243–2245.
23. A. S. Tatikolov, *J. Photochem. Photobiol. C*, 2012, **13**, 55–90.
24. S. Gwon, B. Ananda, H. Kim, Y. Son and S. Kim, *Spectrochim. Acta A*, 2015, **144**, 226–234.
25. Y. Li, F. Wei, Y. Lu, S. He, L. Zhao and X. Zeng, *Dye. Pigment.*, 2013, **96**, 424–429.
26. Y. Li, S. He, Y. Lu and X. Zeng, *Org. Biomol. Chem.*, 2011, **9**, 2606–2609.
27. J. Du, J. Fan, X. Peng, H. Li, J. Wang and S. Sun, *J. Fluoresc.*, 2008, **18**, 919–924.
28. M. Panigrahi, S. Dash, S. Patel and B. K. Mishra, *J. Phys. Chem. B*, 2011, **115**, 99–108.
29. M. Panigrahi, S. Patel and B. K. Mishra, *J. Mol. Liq.*, 2013, **177**, 335–342.
30. H. A. Shindy, *Dye. Pigment.*, 2017, **145**, 505–513.
31. P. Carol, S. Sreejith and A. Ajayaghosh, *Chem. Asian J.*, 2007, **2**, 338 – 348.
32. S. Chowdhury, B. Rooj, A. Dutta and U. Mandal, *J. Fluoresc.*, 2018, **28**, 999–1021.
33. A. T. Afaneh and G. Schreckenbach, *J. Phys. Chem. A*, 2015, **119**, 8106-8116.
34. S. A. McFarland and N. S. Finney, *J. Am. Chem. Soc.*, 2001**, 123**, 1260-1261.
35. E. Lee, S.-H. Shim and M. Cho, *Chem. Sci.*, 2018, **9**, 8325-8336.
36. V. Singh, P. Srivastava, S. Prakashverma, A. Misra, P. Das and N. Singh, *J. Lumin.*, 2014, **154**, 502–510.

37. S. O. Tümay, A. Uslu, H. Ardiç Alidağı, H. H. Kazan, C. Bayraktar, T. Yolaçan, M. Durmuş and S. Yeşilot, *New J. Chem.*, 2018, **42**, 14219–14228.
38. E. Bozkurt and H. I. Gul, *Sensors Actuators, B Chem.*, 2018, **255**, 814–825.
39. B. Paramanik, D. Bain and A. Patra, *J. Phys. Chem. C*, 2016, **120**, 17127–17135.
40. D. Singhal, N. Gupta and A. K. Singh, *RSC Adv.*, 2015, **5**, 65731–65738.
41. R. Sheng, P. Wang, W. Liu, X. Wu and S. Wu, *Sensors Actuators, B Chem.*, 2008, **128**, 507–511.
42. X. Chen, S. W. Nam, M. J. Jou, Y. Kim, S. J. Kim, S. Park and J. Yoon, *Org. Lett.*, 2008, **10**, 5235–5328.
43. H. Dai and H. Xu, *Bioorganic Med. Chem. Lett.*, 2011, **21**, 5141–5144.
44. L. Wang, J. Xiang, H. Sun, Q. Yang, L. Yu, Q. Li, A. Guan and Y. Tang, *Dye. Pigment.*, 2015, **122**, 382–388.
45. G. Zong and G. Lu, *J. Phys. Chem. C*, 2009, **113**, 2541–2546.
46. G. G. Vinoth Kumar, M. P. Kesavan, A. Tamilselvi, G. Rajagopal, J. D. Raja, K. Sakthipandi, J. Rajesh and G. Sivaraman, *Sensors Actuators, B Chem.*, 2018, **273**, 305–315.
47. T. C. Wang, F. Cochet, F. A. Facchini, L. Zaffaroni, C. Serba, S. Pascal, C. Andraud, A. Sala, F. Di Lorenzo, O. Maury, T. Huser and F. Peri, *Bioconjug. Chem.*, 2019, **30**, 1649–1657.
48. S. Zhou, Q. Zhang, X. Tian, G. Hu, F. Hao, J. Wu and Y. Tian, *Dye. Pigment.*, 2012, **92**, 689–695.
49. E. Coronado, J. R. Galán-Mascarós, C. Martí-Gastaldo, E. Palomares, J. R. Durrant, R. Villar, M. Gratzel and M. K. Nazeeruddin, *J. Am. Chem. Soc.*, 2005, **127**, 12351–12356.
50. A. Misra and M. Shahid, *J. Phys. Chem. C*, 2010, **114**, 16726–16739.

Declaration of interests

√☐ The authors declare that they have no known competing financial interests or personal relationships that could have appeared to influence the work reported in this paper.

☐The authors declare the following financial interests/personal relationships which may be considered as potential competing interests: